Reducing the False Rejection Rate of Iris Recognition Using Textural and Topological Features

M. Vatsa, R. Singh, and A. Noore

Abstract—This paper presents a novel iris recognition system using 1D log polar Gabor wavelet and Euler numbers. 1D log polar Gabor wavelet is used to extract the textural features, and Euler numbers are used to extract topological features of the iris. The proposed decision strategy uses these features to authenticate an individual's identity while maintaining a low false rejection rate. The algorithm was tested on CASIA iris image database and found to perform better than existing approaches with an overall accuracy of 99.93%.

Keywords—Iris recognition, textural features, topological features.

I. INTRODUCTION

AMONG the present biometric traits, iris is found to be the most reliable and accurate [1]. The use of human iris as a biometric feature offers many advantages over other biometric features. Iris is the internal human body organ that is visible from outside, but well protected from external modifiers. It has epigenetic formation and it is formed from the individual DNA, but a large part of its final pattern is developed at random. Two eyes from the same individual, although are very similar, contain unique patterns. Similarly, identical twins would exhibit four different iris patterns. These characteristics make it attractive for use as a biometric feature to identify individuals. Pattern recognition and image processing algorithms can be used to extract the unique patterns of iris from an eye image and encode it into an iris template. This iris template contains mathematical representation of the unique information stored in the iris and allows comparisons to be made between templates.

Since 1990s, many researchers have worked on this problem. Human iris recognition process is basically divided into four steps,

- Localization: Inner and outer boundaries of the iris are extracted.
- Normalization: Iris of different people may be of different size. For the same person, the size may vary because of changes in illumination and other factors. So normalization is performed to get all the images in a standard form suitable for processing.
- Feature extraction: Iris provides abundant texture information, a feature vector is formed which consists of the ordered sequence of features extracted from the various representations of the iris images.
- Matching: Feature vectors are classified through different thresholding techniques like Hamming Distance, weight vector and winner selection, dissimilarity function, etc.

Daugman [1, 14] first proposed an algorithm for iris recognition. His algorithm is based on Iris Codes. Integro-differential operators are used to detect the centre and diameter of the iris. The image is converted from cartesian to polar transform and rectangular representation of the region of interest is generated. Feature extraction algorithm uses the complex valued 2D Gabor wavelets [1, 14] to generate the iris codes which are then matched using Hamming Distance. The algorithm gives the accuracy of more than 99.99%. Also the time required for iris identification is less than one second.

Wildes used an isotropic band-pass decomposition derived from the application of Laplacian of Gaussian filters to the image data [2]. Like Daugman [1], Wildes also used the first derivative of image intensity to find the location of edges corresponding to the borders of the iris. Wilde's system explicitly models the upper and lower eyelids with parabolic arcs whereas Daugman excludes the upper and the lower portions of the image. The results of this system were good enough to recognize the individuals in minimum time period.

Boashash and Boles [3] proposed a new approach based on zero-crossings wavelet transform. They first localized and normalized the iris by using edge detection and other well known computer vision algorithms. The zero-crossings of the wavelet transform are then calculated at various resolution levels over concentric circles on the iris. The resulting one dimensional (1D) signals are then compared with the model features using different dissimilarity function. The algorithm is invariant to translation, rotation, scale and illumination and can handle the noisy conditions as well. A similar type of system has been presented in [6] which is based on zero-crossing discrete dyadic wavelet transform representation and has shown a higher level of accuracy.

In [4], the features of iris signals are extracted by Multi-resolution Independent Component Identification (M-ICA). M-ICA provides good properties to represent signals with time frequency. The accuracy obtained is low because the M-ICA does not give good performance on class-separability.

There are some other researchers who have used different algorithms for feature extraction. Dargham *et. al.* [9] used thresholding to detect iris from pupil and the surroundings. The detected iris is reconstructed into a rectangular format and self organizing map networks are then used for recognizing the iris patterns. The accuracy obtained by the network is around 83%. In another approach by Li Ma *et. al.*,

Mayank Vatsa, Richa Singh and Afzel Noore are with the Lane Department of CSEE, West Virginia University, Morgantown, 26505, USA (e-mail: mayankv, richas, noore@csee.wvu.edu).

Multichannel [7] and Even Symmetry Gabor filters [8] are used to capture local texture information of the iris, which are used to construct a fixed length feature vector. Nearest feature line method is used for iris matching. The results obtained were 0.01% for false acceptance rate and 2.17% for false rejection rate. In [10], Chen and Yuan developed the algorithm for extracting the iris features based on fractal dimension. Iris zone is partitioned into small blocks in which local fractal dimension features are computed as the iris code and finally the patterns are matched using the k-means and neural networks. The results obtained are 91.8% genuine acceptance and 100% imposter rejection rate. Zhu *et. al.* [11] used Gabor filters and 2-D wavelet transforms for feature extraction. For identification, weighted Euclidean distance classification has been used. This method is invariant to translation and rotation and tolerant to illumination. The classification rate on using Gabor is 98.3% and the accuracy with wavelets is 82.51%. Tisse *et. al.* [12] used a combination of the integro-differential operators with a Hough Transform for localization and for feature extraction the concept of instantaneous phase or emergent frequency is used. Iris code is generated by thresholding both the models of emergent frequency and the real and imaginary parts of the instantaneous phase. Finally the matching is performed using Hamming distance. 11% false reject rate was obtained by the algorithm. Lim *et. al.* [13] used Haar Wavelet transform to extract features from iris images. By applying the transform four times on image of size 450 x 60 and combining the features, 87 bit feature vector was obtained. For classification of the feature vectors, weight vector initialization and winner selection strategy has been used. The recognition rate obtained is around 98.4%. In [15] two new methods of statistical and computer evaluations of the iris structure have been proposed which are based partly on the correlation analysis and partly on the median binary code of commensurable regions of digitized iris image. Similarly the method of iris structure characterization using statistical and spectral analysis of color iris images is considered in [16]. Gurianov *et.al.* [16] used Wiener spectra for characterization of iris patterns. In [17, 19] human iris structure is explained and classified using coherent Fourier spectra of the optical transmission.

In [22], iris recognition algorithm is presented in which the quality of image is assessed with the help of Support Vector Machines. The detection is done using Hough Transform and the feature vectors are generated using the Multichannel Spatial Filters. The dimensionality reduction of feature vectors is done using Fisher Linear Discriminant and then matching is performed. In [21], vertical, horizontal projections and Hough transform are used for localization followed by Dyadic Wavelet for feature vector generation.

The present day iris recognition systems offer reliable and effective security but these systems are low on user confidence, user friendliness and have a high False Rejection Rate (FRR). In this paper we present a novel iris verification algorithm which uses textural and topological features of the iris image. The proposed 1D log polar Gabor wavelet is used to extract the textural information and Euler numbers are used to extract the topological information from the iris image. We have used hamming distance algorithm [1] and proposed difference matching algorithm to match the textural and topological information. Based on these algorithms, a matching strategy is presented to reduce the false rejection while false acceptance is unaffected. The algorithm is tested on the CASIA iris image database [27].

II. IRIS VERIFICATION

In this section we describe the algorithms proposed for iris verification. An eye image is taken as input from which the iris is detected and converted into polar coordinates. The detected iris image contains noise due to the presence of eyelids and eyelashes. Masking is performed on the polar image to remove the noise. From the masked polar image, templates are generated which are further used for matching. 1D log polar Gabor wavelet and Euler numbers are used to create the iris template and the Euler Code respectively. Next, Hamming Distance (HD) is used to match the iris templates and Directional Difference Matching (DDM) is used for matching Euler Codes. These matching algorithms give the matching scores MS_{IT} for iris template and MS_{EC} for Euler Code respectively. A decision strategy uses these matching scores to compute the acceptance or rejection threshold of the user.

A. Iris Detection

The first stage of iris recognition is the detection of pupil and the iris boundaries from the input eye image. It also involves preprocessing of the iris image to normalize the iris and make it scale invariant.

Detecting Pupil. To find the pupil, a linear threshold is applied on the eye image i.e. pixels with intensity less than a specified empirical value are converted to 0 (black) and pixels greater than or equal to the threshold are assigned 1 (white). Freeman's chain code algorithm [24] is used to find regions of 8-connected pixels having the value 0. It is also possible that eyelashes may satisfy the threshold condition, but they have a much smaller area than the pupil. Using this knowledge, we can cycle through all regions and apply the Freeman's chain code algorithm to retrieve the black pupil in the image. From this region, the central moment is obtained [26]. The edges of the pupil are found by creating two imaginary orthogonal lines passing through the centroid of the region. Starting from the center to both the extremities, boundaries of the binarized pupil are defined by the first pixel with intensity 1.

Finding Iris Boundaries. Next the edges of the iris are determined. The algorithm for finding the edges of the iris from eye image $I(x, y)$ is as follows:

1. Center of pupil (C_{px}, C_{py}) and radius r_p are known using the pupil detection algorithm.
2. Apply Linear Contrast Filter on image $I(x, y)$ to get the linear contrasted image $P(x, y)$.
3. Create vector $A = \{a1, a2,..., aw\}$ that holds pixel intensities of the imaginary row passing through the center of the pupil, with w being the width of the image $P(x, y)$.
4. Create vector R from the vector A which contains elements of A starting at the right fringe of the pupil and ending at the right most element of vector A. Similarly, another vector L is created which contains elements of A
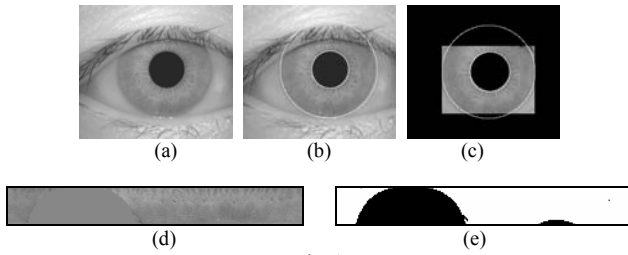
Fig. 1
(a) Original Image (b) Pupil and Iris edges Detected (c) Masked Iris Image
(d) Iris in Polar Coordinates and (e) Corresponding Mask.

starting at the left fringe of the pupil and ending at the left most element of vector *A*.

5. For each side of the pupil (vector *R* for the right side and vector *L* for the left side):
   a. Calculate the average window vector $Avg = \{b1,...,bn\}$ where $n = |L|$ or $n = |R|$. Vector *Avg* is subdivided into *i* windows of size *z*. The value of every element in the window is replaced by the mean value of that window.
   b. Locate the edge point for both the vectors *L* and *R* as the first increment in value of *Avg* that exceeds a threshold *t*.

Thus, the pupil, the iris center, and the radius are calculated and a circle is drawn using these values to locate the pupil and iris edges as shown in Figure 1(b).

Isolating Eyelids and Eyelashes. Eyelids and eyelashes are isolated from the detected iris image considering them as noise because they degrade the performance of the system. The eyelids are isolated by first fitting a line to the upper and lower eyelid using the linear Hough transform. A horizontal line is then drawn which intersects with the first line at the iris edge that is closest to the pupil. A second horizontal line allows the maximum isolation of eyelid regions. Canny edge detection is used to create the edge map, and only the horizontal gradient information is taken. If the maximum in Hough space is lower than a set threshold, then no line is fitted, since this corresponds to non-occluding eyelids. Also, the lines are restricted to lie exterior to the pupil region, and interior to the iris region. A similar process is followed for detecting eyelashes.

Generating Polar Iris Image and its Mask. After detecting the eyelids and the eyelashes, a mask based on the eyelids and eyelashes is used to cover the noisy area and extract the iris without noise as shown in Figure 1(c). Image processing of the eye region is computationally expensive as the area of interest is of donut shape and grabbing the pixels in this region requires repeated rectangular to polar conversion. To simplify this, the iris is first unwrapped into a rectangular region and the pupils are also removed. Let (x, y) be any point on input image with respect to center of pupil, which lies between the inner and the outer boundaries of the iris. Let $f(x, y)$ be the pixel value of point (x, y). Then the corresponding polar coordinates (r, θ) are

$$r = \sqrt{x^2 + y^2}, \theta = \tan^{-1}(y/x) \text{ for } \theta \in (-\pi, \pi] \quad (1)$$

A mask for this polar iris image is generated using the masked iris image shown in Figure 1(c) and the process is

similar to polar iris image generation. Figure 1(d) shows the polar iris image and Figure 1(e) shows the corresponding mask image.

B. Template Generation

This section describes the extraction of textural and topological features from the preprocessed image using 1D log polar Gabor and Euler numbers respectively. The template generated by encoding the textural features is called the iris template and the template from topological features is called the Euler Code.

Iris Texture Template Generation. We propose the use of log polar form of 1D Gabor wavelet for iris texture template. Like Gabor wavelets, log polar Gabor filters are based on polar coordinates but unlike the frequency dependence on a linear graduation, the dependency is realized by a logarithmic frequency scale. Therefore, the functional form of 1D log polar Gabor wavelet is given by:

$$Glp_{r_0\theta_0}(r) = \exp(-2\pi^2\sigma^2(\ln(\frac{r-r_0}{f}))^2\tau^2 \Big/ (2\ln(f_0\sin(\theta-\theta_0))^2 \quad (2)$$

where (r, θ) are the polar co-ordinates, r_0 and θ_0 are the initial values, *f* is the center frequency of the filter and f_0 is the parameter which controls the bandwidth of the filter. σ and τ are defined as follows:

$$\sigma = \frac{1}{\pi \ln(r_0)\sin(\pi/\theta_0)}\sqrt{\frac{\ln 2}{2}} \quad (3)$$

$$\tau = \frac{2\ln(r_0)\sin(\pi/\theta_0)}{\ln 2}\sqrt{\frac{\ln 2}{2}} \quad (4)$$

In contrast to Gabor wavelets which are symmetric with respect to their principal axis, log polar Gabor filters show a translation of maximum from the center of gravity in the direction of a lower frequency and flattening of the high frequency part. The most important feature of the proposed filter is that it is rotation and scale invariant. Also log polar Gabor functions, having extended tails, should be able to encode natural images more efficiently than regular Gabor functions because regular Gabor function would over-represent the low frequency components and under-represent the high frequency components in any encoding process [25]. Figure 2 shows the plot of 1D log polar Gabor transfer function.

To generate an iris template from the proposed 1D log polar Gabor wavelet, the 2D normalized pattern, i.e. polar iris image, is decomposed into a number of 1D signals where each row corresponds to a circular ring on the iris region. The angular direction is used rather than the radial one, which
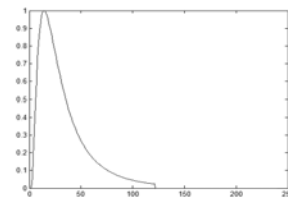

Fig. 2
Log polar Gabor Transfer Function

corresponds to columns of the normalized pattern because maximum independence occurs in the angular direction. These 1D signals are then convolved with the 1D log polar Gabor wavelet in frequency domain. The complex valued output signals are encoded as presented in [1] to generate the iris template. The iris template is a bitwise template containing a number of bits of information, and a noise mask which corresponds to noisy areas within the iris pattern. Figure 3 shows the iris template, its corresponding mask and the
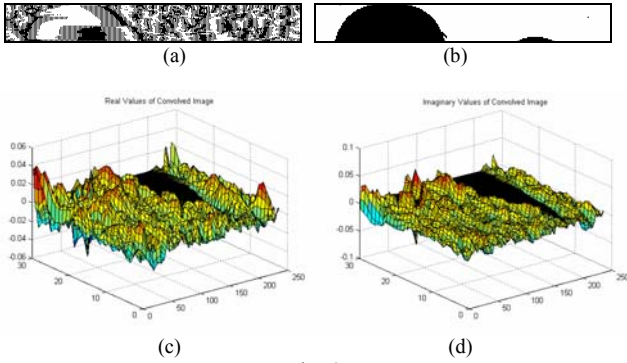

Fig. 3
(a) Iris template (b) Corresponding Mask (c) & (d) Real & Imaginary part of the convolved Iris Image

convolved iris image.

Figure 4 shows the iris code generation process. Figure 4(a) is the input eye image, (b) is the detected inner and outer boundaries, (c) shows the detected iris region, (d) is the mask for the noise present in the image which is applied on the polar image to give masked polar image (e) and (f) is the iris
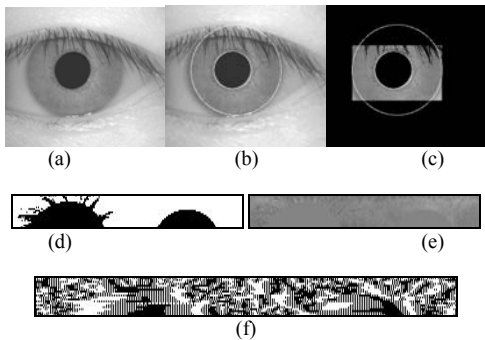

Fig. 4
(a) Eye Image (b) Inner and Outer Boundaries (c) Iris portion in the Eye Image (d) Mask for the Noise present in the Iris Image (e) Mask applied to the Polar Image (f) Iris Template

template generated from log polar Gabor.

Iris Euler Code Generation. For comparing two polar iris images using Euler Code, a common mask is generated. This common mask is obtained by performing a bitwise-OR operation of the two individual masks and is applied to both the polar images. For generating the Euler Code, four binary images corresponding to the four Most Significant Bits (MSB) of the masked polar iris image are considered. As shown in Figure 5, binary images are obtained by considering the four MSBs of every pixel of masked polar iris image separately. The Euler number which represents the difference between the number of connected components and the number of holes

[26] is computed for these binary images. This extracts the topological property of the iris image and is useful for global description of regions in the image. The topological feature is unaffected by common transformation and rotation. Euler Code is a vector matrix consisting of Euler numbers calculated from the four binary images. Figure 6 shows the Euler Codes
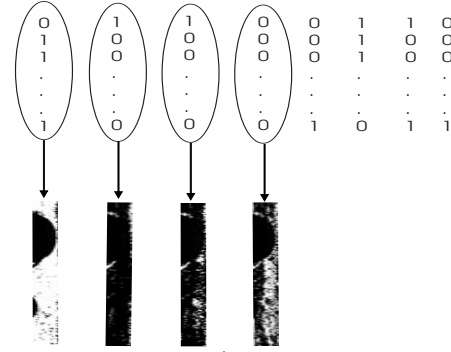

Fig. 5
Generating four binary images from masked polar image

	EULER VECTOR			
IMAGE 1	-72	64	140	-365
IMAGE 2	-62	84	148	-371
IMAGE 3	-63	75	145	-368

Fig. 6
Euler code

of a person at three different instances.

C. Template Matching

To verify a person's identity, we match the calculated iris template with the stored template. Hamming Distance based matching algorithm [1] is used for iris template matching and Vector Difference Matching algorithm is used for Euler Code matching. For the two masked binary templates A_i and B_i, HD can be calculated as:

$$HD = \frac{1}{N}\sum_{i=1}^{N} A_i \oplus B_i \text{ and } MS_{IT} = (1 - HD) \qquad (5)$$

where N is the number of bits represented by each template and $\oplus$ is XOR operation. HD gives the matching score (MS_{IT}) for the iris template as given in Equation 5. For handling the rotation, templates are shifted left and right bit-wise and a number of HD values are calculated from successive shifts [1] and the smallest value is used as the final HD to calculate the matching score. This bit-wise shifting in the horizontal direction corresponds to rotation of the original iris region at an angle given by the angular resolution used. It is capable of taking into account the misalignments in the normalized iris pattern caused by rotational differences during imaging.

The Vector Difference Matching algorithm is designed to match two Euler Codes. In this algorithm, a comparison matrix is created with binary elements. This matrix stores the results of comparison of input Euler Code to the Euler Code from the database. For comparing Euler numbers the following equation is used:

$$|Y_1 - Y_2| \le \varepsilon \qquad (6)$$

where ε is the tolerant error, Y_1 and Y_2 are the Euler numbers from the input Euler Code and the stored Euler Code respectively. The comparison matrix is initialized with all zeros. If the difference between Y_1 and Y_2 is less than the tolerant error ε then a one is entered in the comparison matrix. Figure 7 illustrates the procedure for generating the comparison matrix when the input is from a genuine user and an imposter (at $\varepsilon = 20$).

	EULER VECTOR			
INPUT	-72	64	140	-365
DATABASE	-62	74	148	-371
COMPARISON	1	1	1	1

(a)

	EULER VECTOR			
INPUT	-72	64	140	-365
DATABASE	12	98	-28	118
COMPARISON	0	0	0	0

(b)

Fig. 7
Illustrating generation of comparison matrix (a) Genuine (b) Impostor

For matching using the comparison matrix, the number of one's and zero's are counted. If all are one's then it is a match and if all are zero's then it is a mismatch. Although, ideally two Euler Codes generated from the same iris should have a comparison matrix of all one's, practically it does not happen because of the noise introduced at various stages. So, we calculate matching score (MS_{EC}) of Euler Code based on the comparison matrix as shown in Equation 7.

$$MS_{EC} = Non\text{-}Zero\text{-}values\,(Comparison\ Matrix)\,/\,4 \quad \textbf{(7)}$$

D. Decision Strategy

Iris recognition systems and algorithms have succeeded in achieving a low false acceptance rate but the rejection rates have remained high. False rejection rate should be as low as possible to make the iris recognition system more practical and adaptable to diverse applications. A template database is prepared as shown in Figure 8(a). For getting enrolled in the database at least 70% of iris information should be present, i.e. the noise in the image due to eyelids and eyelashes or the total area covered by the mask should be less than 30%. In the database, templates from three images of an individual are stored. For verifying the identity of an individual, the eye image is detected and if more than 35% of the noise area is present then the image is not suitable for matching. From the query polar iris image, features are encoded and then the iris templates and Euler Codes are matched using the matching algorithms. A decision strategy is followed as shown below:

1. If all the three MS_{IT} are less than a threshold, *thresh-hd-min*, then the person is accepted.
2. If all the three MS_{IT} are greater than a threshold, *thresh-hd-max*, then the person is rejected.
3. If both the above conditions are not satisfied then:
   a. Sort the three matching scores in descending order and apply the following equation to get a new matching score MS_{IT-New}:

$$MS_{IT-New} = (s1 * MS_{IT(\max)} + s2 * MS_{IT(mid)} + s3 * MS_{IT(\min)})/(s1 + s2 + s3) \quad \textbf{(8)}$$

where $s1$, $s2$ and $s3$ are three empirical values such that $s1 > s2 > s3$. This equation gives more weight to the matching score by which a user is accepted and less to the matching score by which a user is rejected.

b. Calculate MS_{EC-Avg}, average value of the three matching score of Euler Codes.

c. If MS_{IT-New} and MS_{EC-Avg} are greater than thresholds, *thresh-hd-new*, and, *thresh-ec-avg*, then the person is accepted; otherwise the person is rejected.

For our experiments, the values of the matching scores are, *thresh-hd-min* is 0.36, *thresh-hd max* is 0.40, s1, s2, and s3 are 0.3, 0.3 and 0.1 respectively. The value of *thresh-hd-new* is set to be 0.38 and *thresh-ec-avg* is 2. Figure 8 shows the database enrollment and matching strategies.
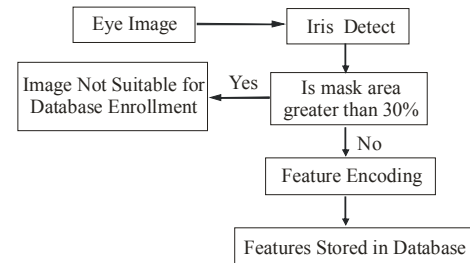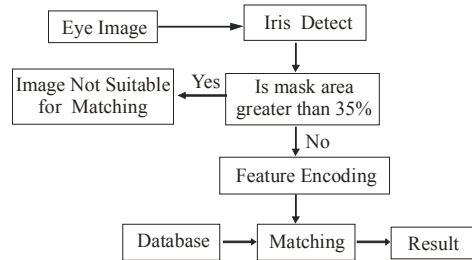
Fig. 8
(a) Database Enrollment and (b) Matching Strategy of Iris Recognition System

III. EXPERIMENTAL RESULTS

The proposed algorithms are tested on the CASIA iris image database [27]. Using CASIA database, we have iris images from 306 different iris classes. To test the proposed algorithm using these images we have 28,560 possible cases to check the false rejection and 2,17,770 possible cases for false acceptance. Different performance factors and thresholds are carefully chosen after intensive experimental evaluations to get the best performance.

The iris detection process shows good performance and we found that only in two instances the detection algorithm fails to detect the iris region properly. Figure 9 shows the detection result on these two instances. The algorithm fails in the first instance because the upper eye-lashes causes a steep intensity variation and an edge point is marked at this position. In the other case, there is a sharp variation in the iris pattern due to

the lighting conditions and this causes the edge point marked much before the actual edge point.
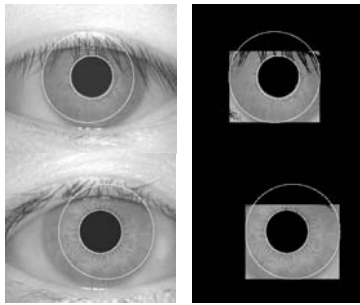

Fig. 9
Images showing failure of detection

According to the decision strategy, if the noise present in iris image is more than 30%, then the image is not suitable for enrollment. In the experiments, we found that this step is accurately handled by the algorithm. Figure 10 shows the examples in which the algorithm correctly discards such images. Also, there are no cases where the algorithm discards a good quality image (noise present in the image is less than 30%) or allows a bad image (noise present in the image is more than 30%).
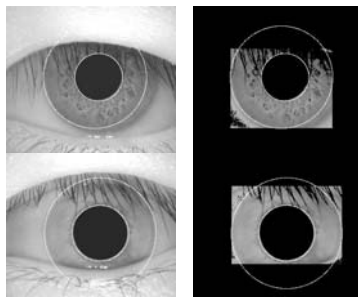

Fig. 10
Images with noise greater than 30%

The verification performance of the proposed iris recognition algorithm is evaluated assuming that there is 0% false enrollment rate, i.e. enrollment process contains only the genuine users with images having less than 30% of noise. Figure 11(a) shows the intra-class and inter-class distance distribution plot of Hamming Distance calculated by the proposed 1D log polar Gabor wavelet and Figure 11(b) shows the ROC curve of the proposed decision strategy. The accuracy (Accuracy = $100 - (FAR+FRR)/2$) of the iris verification system is 99.93%, with zero false acceptance (out of 2,17,770 cases) and 95 false rejection cases (out of 28,560 cases). When using only 1D log polar Gabor wavelet there is zero false acceptance and 239 cases for false rejection. This shows that the proposed decision algorithm reduces the false rejection rate.

We also performed experiments on storing multiple iris templates in the database. We calculated FRR at 0% FAR for the varying size of database template from one to six. Figure 12 shows that by increasing the number of training templates the FRR decreases and after 3 training samples it becomes approximately constant. Thus using three templates in the database we are able to predict the behavior of intra-class
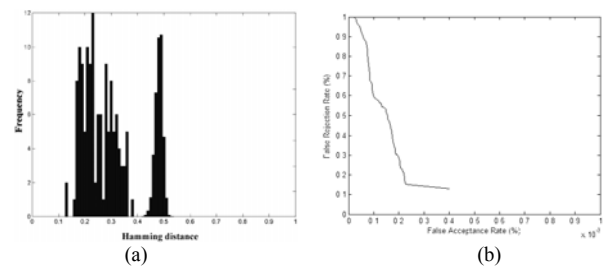

Fig. 11
(a) Inter-class and Intra-class Distance Distribution Plot using 1D log polar Gabor Wavelet and (b) ROC curve of Proposed Decision Strategy

distribution more accurately and therefore work better than single-template.

In this paper we also compared the accuracy and the error rates of the proposed iris verification algorithm with the algorithms proposed by Daugman [1], Li *et. al.* [21] and Tan *et al.* [22] using the CASIA iris image database [27].
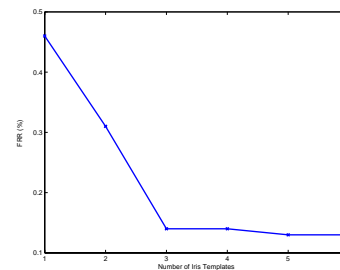

Fig. 12
FRR vs Number of training sample

Table 1 shows the verification accuracy of the algorithms. The experimental results illustrate that the proposed algorithm is much better than the algorithms proposed in [21] and [22] and is comparable with Daugman's algorithm [1]. This comparison also justifies the use of the proposed log polar Gabor wavelet, Euler codes and decision strategy in compared to other forms of Gabor wavelet as proposed in [21] and [22].

TABLE I
PERFORMANCE COMPARISON OF THE ALGORITHMS

ALGORITHM/	FAR (%)	FRR (%)	ACCURACY (%)
Daugman [1]	0.00	0.13	99.94
Li M. *et. al.* [21]	0.00	0.87	99.57
Tan *et. al.* [22]	0.00	1.03	99.49
Proposed System	0.00	0.14	99.93

V. CONCLUSION

In this paper a novel iris recognition system is proposed considering both the textural and topological features of an iris image to reduce the false rejection rates. The proposed 1D log polar Gabor wavelet is applied on a transformed polar iris image to extract textural features and Euler numbers are used to extract the topological features. A decision strategy is proposed to verify the authenticity of an individual. Experimental results show that the proposed system is capable of reducing the false rejection cases with zero false acceptances. Also, the proposed system is compared with the

existing algorithms and the performance is highly suitable for real time applications.

ACKNOWLEDGEMENT

REFERENCES

[1] J. G. Daugman, "High Confidence Visual Recognition of Persons by a Test of Statistical Independence", *IEEE Transactions on Pattern Analysis and Machine Intelligence,* Vol.15, No. 11, pp. 1148–1161, 1993.

[2] R. P. Wildes, "Iris Recognition: An Emerging Biometric Technology," Proceedings of the IEEE, Vol. 85, No. 9, 1999, pp. 1348-1363.

[3] W. W. Boles and B. Boashash, "A Human Identification Technique Using Images of the Iris and Wavelet Transform*", IEEE Transactions on Signal Processing*, Vol. 46, No. 4, 1998, pp. 1185-1188.

[4] N. Seung-In, P. Kwanghuk, L. Chulhan and K. Jaihie**, "**Multiresolution Independent Component Identification", *Proceedings of the 2002 International Technical Conference on Circuits/Systems, Computers and Communications*, 2002.

[5] C. H. Daouk, L. A. El-Esber, F. D. Kammoun, and M. A. Al-Alaoui, "Iris Recognition", *Proceedings of the 2nd IEEE International Symposium on Signal Processing and Information Technology*, 2002 pp. 558-562.

[6] C. Sanchez-Avila, R. Sanchez-Reillo and D. de Martin-Roche, "Iris Recognition for Biometric Identification Using Dyadic Wavelet Transform Zero-Crossing"**,** *Proceedings of the IEEE 35th International Carnahan Conference on Security Technology*, 2001, pp. 272 -277.

[7] L. Ma, T. Tan and Y. Wang., "Iris Recognition Based on Multichannel Gabor Filtering", *Proceedings of the International Conference on Asian Conference on Computer Vision*, 2002, pp. 1-5.

[8] L. Ma, T. Tan and Y. Wang, "Iris Recognition Using Circular Symmetric Filters", *International Conference on Pattern Recognition*, Vol.2 , 2002, pp. 414 -417.

[9] J. A. Dargham, A. Chekima, C. F. Liau and W. Lye, "Iris Recognition Using Self- Organizing Neural Network", *Student Conference on Research and Development*, 2002, pp. 169 -172.

[10] W.-S. Chen and S.-Y. Yuan, "A Novel Personal Biometric Authentication Technique Using Human Iris Based on Fractal Dimension Features", *Proceedings of the International Conference on Acoustics, Speech and Signal Processing*, Vol. 3, 2003, pp. 201-204.

[11] Y. Zhu, T. Tan and Y. Wang, "Biometric Personal Identification Based on Iris Patterns", *Proceedings of the IEEE International Conference on Pattern Recognition*, 2000, pp. 2801-2804.

[12] C.-L. Tisse and L. Michel Torres, "Robert, Person Identification Technique Using Human Iris Recognition", *Proceedings of the 15th International Conference on Vision Interface*, 2002, pp. 294-299.

[13] S. Lim, K. Lee, O. Byeon, T. Kim, "Efficient Iris Recognition through Improvement of Feature Vector and Classifier", *Journal of Electronics and Telecommunication Research Institute*, Vol. 23, No. 2, 2001, pp. 61 – 70.

[14] J. G. Daugman, "Statistical Richness of Visual Phase Information: Update on Recognizing Persons by Iris Patterns", *International Journal of Computer Vision*, Vol. 45, No. 1, 2001, pp. 25 – 38.

[15] L. Machala and J. Pospisil, "Alternatives of the Statistical Evaluation of the Human Iris Structure", *Proceedings of the SPIE*, Vol. 4356, 2001, pp. 385-393.

[16] E. V. Gurianov, D. A. Zimnyakov and V. A. Galanzha, "Iris Patterns Characterization by Use of Wiener Spectra Analysis: Potentialities and Restrictions", *Proceedings of the SPIE*, Vol. 4242, 2001, pp. 286-290.

[17] K. Petr, A. Muron and P. Jaroslav, "Human Iris Structure by the Method of Coherent Optical Fourier Transform", *Proceedings of the SPIE*, Vol. 4356, 2001, pp. 394-400.

[18] V. Della, A. Michael, T. Chmielewski, T. A. Camus, M. Salganicoff and M. Negin, "Methodology and Apparatus for Using the Human Iris as a Robust Biometric", *Proceedings of the SPIE*, Vol. 3246, 1998, pp. 65-74.

[19] A. Muron, K Petr. and P. Jaroslav, "Identification of Persons by Means of the Fourier Spectra of the Optical Transmission Binary Models of the Human Irises", *Optics Communications*, Vol. 192, 2001, pp. 161-167.

[20] J. M. H. Ali and A. E. Hassanien, "An Iris Recognition System to Enhance E-security Environment Based on Wavelet Theory", *AMO - Advanced Modeling and Optimization*, Vol. 5, No. 2, 2003, pp. 93-104.

[21] L. Ma, T. Tan, Y. Wang and D. Zhang, "Efficient Iris Recognition by Characterizing Key Local Variations", *IEEE Transactions on Image Processing*, Vol. 13, No. 6, 2004, pp. 739-750.

[22] T. Tan, L. Ma, Y. Wang and D. Zhang, "Personal Identification based on Iris Texture Analysis", *IEEE Transactions on Pattern Analysis and Machine Intelligence*, Vol. 25, No. 12, 2003, pp. 1519-1533.

[23] B. R. Meena, M. Vatsa, R. Singh and P. Gupta, "Iris Based Human Verification Algorithms", *Proceedings of International Conference on Biometric Authentication*, 2004, pp. 458-466.

[24] H. Freeman, "Computer Processing of Line - Drawing Images", *Computer Surveys*, Vol. 6, No. 1, 1974, pp. 57-97.

[25] C. Palm and T. M. Lehmann, "Classification of Color Textures by Gabor Filtering", *Machine Graphics and Vision*, Vol. 11, No. 2/3, 2002, pp. 195-219.

[26] Gonzalez and Woods, (2001), *Digital Image Processing*, Second Edition, Pearson Education.

[27] http://nlpr-web.ia.ac.cn/english/irds/irisdatabase.htm

Mayank Vatsa is a graduate research assistant in the Lane Department of Computer Science and Electrical Engineering at West Virginia University. He is currently pursuing his Doctoral degree in Computer Science. He had been actively involved in the development of a multimodal biometric system which includes face, fingerprint and iris recognition at Indian Institute of Technology Kanpur, India from July 2002 to July 2004. His current areas of interest are pattern recognition, image and video processing, biometric authentication, watermarking and information fusion.

Richa Singh is a graduate research assistant in the Lane Department of Computer Science and Electrical Engineering at West Virginia University. She is currently pursuing her Doctoral degree in Computer Science. She had been actively involved in the development of a multimodal biometric system which includes face, fingerprint and iris recognition at Indian Institute of Technology Kanpur, India from July 2002 to July 2004. Her current areas of interest are pattern recognition, image processing, neural networks, biometric authentication, watermarking, and data fusion.

Afzel Noore received his Ph.D. in Computer Engineering from West Virginia University in 1987. From 1980 to 1983, he worked as a digital design engineer at Philips India and developed microprocessor based multimeters in collaboration with Philips Eindhoven Holland. He is an Associate Professor in the Lane Department of Computer Science and Electrical Engineering. He served as the Associate Dean for Academic Affairs and Special Assistant to the Dean in the College of Engineering and Mineral Resources at West Virginia University from 1996 to 2003,. His research interests include biometrics, digital watermarking, computational intelligence, fuzzy and neural systems, fault-tolerant computing, software reliability, and consumer electronics. His research has been funded by Westinghouse, GE, NSF, Electric Power Research Institute, Department of Energy, NASA and the US Department of Justice.